Univerzitet u Beogradu
Publikacije Elektrotehničkog Fakulteta
Serija Tehnička fizika (1996), 26–42

WAVES IN RELATIVISTIC PLASMAS Part I: Wave propagation perpendicular to the magnetic field

S. Pešić and Lj. Nikolić

"Vinča" Institute for Nuclear Sciences, Laboratory for Nuclear and Plasma Physics, P.O.B. 522, 11001 Belgrade, Yugoslavia

The propagation and absorption properties of waves in fully relativistic plasmas are examined. In the present, first part of the paper, the results of the analysis of ordinary and extraordinary wave propagation perpendicular to an external magnetic field, are presented. Several interesting effects introduced by the relativistic mass increase associated with increasing the electron temperature, are discussed. In particular, it is found that the cutoff density of ordinary waves enlarges significantly with the increase of the electron temperature. The effects of anomalous wave dispersion which appear near the fundamental electron cyclotron frequency and its second and third harmonic are largest for low temperatures and subsist up to the intermediate temperatures ($T \approx 300$ keV). An efficient damping of ordinary waves is obtained in a wide temperature range. The harmonic structure of the absorption profiles and the effects of anomalous dispersion almost simultaneously disappear. Relativistic effects increase the magnetic field at which the extraordinary wave is cut off. The largest relative shifts of the location of the right-hand cutoff occurs near the electron cyclotron frequency. In the range of intermediate electron temperatures, the right-hand cutoff of the extraordinary wave disappears. The phenomenon of mode coupling near the second harmonic of the electron cyclotron frequency is examined in details, in a wide electron density and temperature ranges. The results of the present fully relativistic analysis confirm and complement the previously reported ones on this phenomenon. Both, the electromagnetic and electrostatic modes are efficiently damped near the upper hybrid resonance. Finally, it is concluded that the obtained results may have important implications for the wave absorption and in particular, emission in relativistic plasmas.

I Introduction

The wave particle interaction around the electron cyclotron frequency and its first few harmonics has been extensively investigated both, experimentally and theoretically because of its relevance to the plasma heating in fusion devices, current drive and plasma diagnostics. It has been demonstrated

that the relativistic variation of electron mass with energy profoundly modifies the wave particle interaction process, and in a majority of considered cases, it makes inadequate the results obtained by using nonrelativistic approximations. Although electron temperatures measured in present-day fusion devices remain small ($T \leq 15$ keV) relative to the rest mass energy of the electrons (511 keV), recent investigations have revealed significant relativistic effects. The relativistic mass variation introduces, among others, resonance broadening and shifting of the absorption profiles, wave absorption (or emission) at propagation perpendicular to the external magnetic field, shifts in the locations of cutoffs, etc. Most of the previous theoretical work has been done within the weakly relativistic approximation that is, by considering thermal plasma in the regime $T \ll mc^2$ (m is the rest mass and c is the velocity of light). The range of its applicability depends strongly on the electron temperature and wave frequency or more precisely, on the order on which finite Larmor radius effects are retained in the dielectric tensor. The temperature at which the weakly relativistic approximation breaks down ranges from about 10 keV to 20 keV. The wave propagation in a fully relativistic plasmas is considered only in a limited number of cases [1] - [3]: *(i)* perpendicular wave propagation and *(ii)* by assuming a real wave refractive index, wave propagation oblique with respect to the external magnetic field. Due to the wave-particle interaction which can be very strong near the electron cyclotron resonance, in general the dielectric tensor is non-Hermitian. As known, absorption (or emission) arises only from the non-Hermitian part of the dielectric tensor. So, the dispersion equation governing the waves in the plasma has to be considered as a complex equation having complex roots. Since we are primarily interested in propagation and damping of waves (externally) launched at some (real) frequency, here the wave dispersion equation is treated as an expression for the functional dependence of the complex wave refractive index N upon the dimensionless parameters: the electron density $X = \omega_p/\omega$, the magnetic field $Y = \omega_c/\omega$ and the temperature T (ω is the wave frequency, ω_p and ω_c are the electron plasma and cyclotron frequencies, respectively). This permits to analyse the wave spatial damping in relativistic plasmas and in particular, in domains of parameters of practical interest that have not been explored before. Preliminary results have recently been reported in [4,5].

The paper is divided into two parts. In the present, first part, wave propagation (strictly) perpendicular to an external magnetic field $\vec{B}_0 = B_0\vec{e}_z$ in a fully relativistic plasma is considered. The Part II will contain the analysis of oblique wave propagation. In Section 2 we first discuss the dispersion equation that governs waves propagating in a fully relativistic thermal magnetized plasma. We also briefly outline the development of an alternate, nonstandard approach [3] to the calculation of the dielectric tensor of fully relativistic plasma which is efficiently applied in the present paper. In Section 3 we present solutions of the fully relativistic and, for reason of comparison, of the weakly relativistic dispersion equation, for various electron densities and temperatures indicating the propagation and absorption properties of ordinary wave in the frequency range covering the fundamental EC frequency and its first few harmonics. The results of the analysis of the extraordinary wave propagation in a fully relativistic plasma are presented in Section 4. Finally, the obtained results are summarized and conclusions discussed in Section 5.

II General dispersion equation

The dispersion relation governing waves with circular frequency ω propagating in a homogeneous plasma confined by a steady magnetic field has a general form

$$D(\vec{N},\omega) = \left[N_iN_j - N^2\delta_{ij} + \varepsilon_{ij}\right] = 0 \ , \tag{1}$$

where ε_{ij} is the element of the corresponding dielectric tensor and δ_{ij} is the Kronecker's symbol. Local symmetry around the direction of the magnetic field implies that the dispersion relation is a function of the wave refractive index only through $N_\perp$ and $N_{||}$ that is, $D(\vec{N},\omega) = D(N_\perp, N_{||}, \omega)$. The electromagnetic properties of the considered plasma are completely described by the dielectric tensor. Here, in deriving the general expression for the dielectric tensor for relativistic plasma, we shall not follow the standard mathematical procedure which leads to the Trubnikov formulae [6]. Instead

we shall present an outline of the development proposed by Weiss [3] which has some advantages in computing the dielectric tensor. The starting point is the relativistic collisionless Boltzmann equation that is, the Vlasov equation. The Fourier transform in both time and space, of this equation can be written as,

$$i(\omega - \vec{k}\cdot\vec{v})f_1 + \omega_c(\vec{v}\times\vec{e}_z)\cdot\frac{\partial f_1}{\partial\vec{u}} = -\frac{\omega_p^2\epsilon_0}{e}\left(\vec{E} + \vec{v}\times\vec{B}_1\right)\cdot\frac{\partial f_0}{\partial\vec{u}} \quad , \tag{2}$$

where $\vec{k}$ is the wave number, ϵ_0 is the vacuum dielectric constant, $\vec{v}$ is the electron velocity, $\vec{E}$ is the electric field, $\gamma = 1/(1 - v^2/c^2)^{1/2} = (1 + u^2/c^2)^{1/2}$, $\vec{u} = \gamma\vec{v}$, $f_1(p,t)$ and $\vec{B}_1$ are the first order peturbation of the equilibrium electron momentum distribution $f_0 = f_0(p)$ and magnetic field $\vec{B}_0$, respectively. Note that the distribution function is a function of momentum (p) rather than velocity. At this point, we take the usual coordinate system,

$$\vec{B}_0 = (0, 0, B_0) \quad ,$$

$$\vec{k} = (0, k_\perp, k_\parallel) \quad ,$$

$$\vec{v} = (v_\perp\cos\phi, v_\perp\sin\phi, v_\parallel) \quad .$$

By developing some of the terms in equation (2), we obtain the following linear first order differential equation for $f_1(p)$

$$i(\omega - \vec{k}\cdot\vec{v})f_1 + \omega_c(\vec{v}\times\vec{e}_z)\cdot\frac{\partial f_1}{\partial\vec{u}} = -2\frac{\omega_p^2\epsilon_0}{e}\vec{E}\cdot\vec{u}\frac{\partial f_0}{\partial u^2} \quad , \tag{3}$$

The solution that satisfies the above equation and the condition of periodicity $f_1(\phi) = f_1(\phi + 2\pi)$ can be written in the form,

$$\begin{aligned} f_1 &= \frac{2\omega_p^2\epsilon_0\gamma f_0'}{ec\omega_c}\frac{e^{i(\omega^*\phi + \bar{k}_\perp\bar{u}_\perp\cos\phi)}}{e^{-i2\pi\omega^*} - 1}\int_\phi^{\phi+2\pi}\left(\bar{u}_\perp e^{i\phi'}E_- + \bar{u}_\perp e^{-i\phi'}E_+ + \bar{u}_\parallel E_\parallel\right) \\ &\times\ e^{-i(\omega^*\phi' + \bar{k}_\perp\bar{u}_\perp\cos\phi')}d\phi' \quad , \end{aligned} \tag{4}$$

where

$$\frac{\omega}{\omega_c} = \bar{\omega} \ , \quad \frac{k_\parallel c}{\omega_c} = \bar{k}_\parallel \ , \quad \frac{k_\perp c}{\omega_c} = \bar{k}_\perp \ , \quad \frac{\vec{u}}{c} = \vec{\bar{u}},$$

$$\omega^* = \bar{\omega}\gamma - \bar{k}_\parallel\bar{u}_\parallel \quad .$$

We need to determine the mean current density whose perpendicular and parallel components are

$$J_\pm = -e\int\frac{1}{2}(v_x \pm iv_y)f_1 d^3p \quad ,$$

$$J_\parallel = -e\int v_z f_1 d^3p \quad ,$$

from which we can construct the effective dielectric tensor $\hat{\epsilon}$ and obtain the dispersion equation. The components of the current density can be expressed through integrals whose integrand is a product of two Bessel functions [3],

$$\begin{pmatrix} J_+ \\ J_- \\ J_\parallel \end{pmatrix} = -\frac{i\pi^2\omega_p^2\epsilon_0}{\omega_c}\int_0^\infty\bar{u}_\perp d\bar{u}_\perp\int_{-\infty}^\infty d\bar{u}_\parallel\frac{\bar{f}_0'}{\sin\pi\omega^*}\hat{M}\begin{pmatrix} E_+ \\ E_- \\ E_\parallel \end{pmatrix} \quad , \tag{5}$$

with

$$\hat{M} = \begin{pmatrix} -\bar{u}_\perp^2 J_{\omega^*+1}J_{-\omega^*-1} & \bar{u}_\perp^2 J_{\omega^*+1}J_{-\omega^*+1} & i\bar{u}_\perp\bar{u}_\parallel J_{\omega^*+1}J_{-\omega^*} \\ \bar{u}_\perp^2 J_{\omega^*+1}J_{-\omega^*+1} & -\bar{u}_\perp^2 J_{\omega^*-1}J_{-\omega^*+1} & i\bar{u}_\perp\bar{u}_\parallel J_{\omega^*}J_{-\omega^*+1} \\ -2i\bar{u}_\perp\bar{u}_\parallel J_{\omega^*+1}J_{-\omega^*} & -2i\bar{u}_\perp\bar{u}_\parallel J_{\omega^*}J_{-\omega^*+1} & 2\bar{u}_\parallel^2 J_{\omega^*}J_{-\omega^*} \end{pmatrix},$$

and

$$\vec{f}_0 = m^3c^3\frac{\partial f_0}{\partial \bar{u}^2} \ .$$

As one can see, the integration variables, the perpendicular and parallel components of the particle momentum, appear both in the argument of the Bessel functions and in their index. The dielectric tensor of plasma whose equilibrium particle distribution function is close to the relativistic Maxwellian distribution

$$f_0 = \frac{\mu}{4\pi m^3c^3K_2(\mu)}e^{-\mu\gamma} \ , \tag{6}$$

($K_2(\mu)$ is the modified Bessel function of the second kind (Mac Donald function), $\mu = mc^2/k_BT$, k_B is the Boltzman's constant) can be expressed as a sum of two matrices, $\hat{\epsilon} = \hat{\epsilon}^H + \hat{\epsilon}^A$, where

$$\hat{\epsilon}^H = \hat{I} + \frac{\pi\bar{\omega}_p^2\mu^2}{8K_2(\mu)\bar{\omega}^3}\int_{-1}^{1}d\tilde{u}\frac{1}{(1-N_{||}\tilde{u})^2}\mathbf{P}\int_{\omega^*_{\min}}^{\infty}\omega^*\frac{e^{-\mu\frac{\omega^*}{\bar{\omega}(1-N_{||}\tilde{u})}}}{\sin(\pi\omega^*)}\hat{T}\,d\omega^* \ , \tag{7}$$

$$\hat{\epsilon}^A = -\frac{i\pi\bar{\omega}_p^2\mu^2}{8K_2(\mu)\bar{\omega}^3}\int_{-1}^{1}d\tilde{u}\frac{1}{(1-N_{||}\tilde{u})^2}\int_{\omega^*_{\min}}^{\infty}(-1)^n\delta(\omega^*-n)\omega^*e^{-\mu\frac{\omega^*}{\bar{\omega}(1-N_{||}\tilde{u})}}\hat{T}\,d\omega^* \ . \tag{8}$$

The elements of the matrice $\hat{T}$ are defined as,

$$\begin{aligned}
T_{xx} &= C^2\left(J_{\omega^*+1}J_{-\omega^*-1} + J_{\omega^*-1}J_{-\omega^*+1} - 2J_{\omega^*+1}J_{-\omega^*+1}\right) \ , \\
T_{yy} &= C^2\left(J_{\omega^*+1}J_{-\omega^*-1} + J_{\omega^*-1}J_{-\omega^*+1} + 2J_{\omega^*+1}J_{-\omega^*+1}\right) \ , \\
T_{zz} &= -4G^2J_{\omega^*}J_{-\omega^*} \ , \\
T_{xy} &= -T_{yx} = iC^2\left(J_{\omega^*+1}J_{-\omega^*-1} - J_{\omega^*-1}J_{-\omega^*+1}\right) \ , \\
T_{xz} &= -T_{zx} = -i2CG\left(J_{\omega^*+1}J_{-\omega^*} + J_{\omega^*}J_{-\omega^*+1}\right) \ , \\
T_{yz} &= T_{zy} = -2CG\left(J_{\omega^*+1}J_{-\omega^*} - J_{\omega^*}J_{-\omega^*+1}\right) \ .
\end{aligned}$$

Furthermore, in expression (7) – (8) $\mathbf{P}$ denotes a Cauchy principal value, $\bar{\omega}_p = \omega_p/\omega_c$, $\omega^*_{\min} = \bar{\omega}(1 - N_{||}\tilde{u})/(1-\tilde{u}^2)^{1/2}$, $C = \left(\omega^{*2}/\omega^{*2}_{\min} - 1\right)^{1/2}$, $G = \omega^*\tilde{u}/\bar{\omega}(1-N_{||}\tilde{u})$ and $J_\nu = J_\nu(N_\perp\bar{\omega}C)$ is the ordinary Bessel function of the first kind.

It should be noted that the expressions (7) – (8) for the dielectric tensor differ from the standard ones which contain an integration either with respect to a variable in momentum space, e.g. the momentum parallel to the magnetic field, or with respect to time, depending on whether one starts from the first or second of Trubnikov's formulae [6]. The standard procedure then leads to an infinite sum of terms, each of which contains a Bessel function of the momentum and has to be integrated over the momentum space. The fact that for increasing the particle temperature, the number of harmonics required to give an acceptable accuracy significantly increases, represents a major drawback of the standard procedure.

The dispersion equation governing electromagnetic waves in a relativistic thermal magnetized plasma (or in weakly inhomogeneous plasma located in a magnetic field whose direction is perpendicular to the density, magnetic field and temperature gradients) can be expressed from (1) as,

$$\det\begin{pmatrix} \epsilon_{xx} - N_\perp^2 - N_{||}^2 & \epsilon_{xy} & \epsilon_{xz} \\ -\epsilon_{xy} & \epsilon_{yy} - N_{||}^2 & \epsilon_{yz} + N_\perp N_{||} \\ -\epsilon_{xz} & \epsilon_{yz} + N_\perp N_{||} & \epsilon_{zz} - N_\perp^2 \end{pmatrix} = 0 \ . \tag{9}$$

Since the dielectric tensor elements ϵ_{ij} are transcedental functions on $N_\perp$ and $N_{||}$, the dispersion equation (9) has, in general, an infinite number of roots. Two of them are long wavelength modes and in the cold plasma limit are usually referred to as the extraordinary (X) and ordinary (O) electromagnetic

modes. In the special cases of perpendicular ($N_{||} = 0$) or parallel ($N_{\perp} = 0$) wave propagation, equation (9) splits into two equations describing the propagation of two decoupled fundamental electromagnetic waves. For $N_{||} = 0$ the first equation

$$N_O^2 = \epsilon_{zz} \quad , \tag{10}$$

describes the ordinary wave whose electric field is parallel to the external magnetic field and the second one,

$$N_X^2 = \epsilon_{xx} + \frac{\epsilon_{xy}^2}{\epsilon_{yy}} \quad , \tag{11}$$

describes the extraordinary wave whose electric field is perpendicular to the external magnetic field. Both waves are purely transverse and linearly polarized in the vacuum limit. As we shall see, in plasma the O wave remains linearly polarized while the X wave develops a longitudinal component. In what follows, the two principal electromagnetic waves propagating (strictly) perpendicular to the external magnetic field are labelled as the extraordinary (or X) and the ordinary (or O) wave. At oblique wave propagation the two principal electromagnetic modes which in the limit $N_{||} \to 0$ go over into the aforementioned X and O wave, are labelled as the extraordinary (or X) and ordinary (or O) modes. For $N_{\perp} = 0$, the axial symmetry of the problem imposes that both waves are transverse and circularly polarized, in the plasma as in the vacuum,

$$N_{\pm}^2 = \epsilon_{xx} \pm \epsilon_{xy} \quad . \tag{12}$$

The wave whose refractive index is N_+ is a right-handed polarized wave and its electric field turns around in the direction of gyration of electrons, while the left-handed polarized wave N_- gyrates in the direction of the ion Larmor motion.

Due to the wave-particle interaction which can be very strong near the particle and wave resonances, in general the dielectric tensor is non-Hermitian. As known, absorption (or emission) arises only from the non-Hermitian part of the dielectric tensor. So, dispersion equations (9)–(12) have to be considered as a complex equations.

In practice, the waves are externally launched at some (real) frequency ω by a structure (horn antenna, etc.) which determines the spectrum of the wave refractive index in the direction of the magnetic field $N_{||}$. So, in the case of oblique wave propagation, equation (9) is treated as an expression for the functional dependence of the complex perpendicular component of the wave refractive index $N_{\perp}$ upon the dimensionless parameters X, Y, T and $N_{||}$. Note the convention used in the present paper of the index r denoting the real part of a complex quantity (e.g. $N_r \equiv \mathrm{Re}N$) and the index i denoting the imaginary part of a complex quantity (e.g. $N_i \equiv \mathrm{Im}N$).

Equations (9) – (11) with the tensor component ε_{ij} (7) – (8) are solved numerically in a wide range of the aforementioned dimensionless parameters. The frequency range of interest is centered at the EC frequency and therefrom, the ion dynamics is neglected in (9) – (11). In order to compare the present results with those obtained within the weakly relativistic approximation, we have also developed a code in which the dielectric tensor is expressed through the weakly relativistic dispersion function [7]. It should be noted that in this code finite Larmor radius terms are retained up to the third order.

III Ordinary wave

From the dispersion equation for the ordinary wave (10) one concludes that this wave has no resonance and that in the cold plasma limit, it has the so-called plasma cutoff, $X_c = 1$. The temperature dependence of the ordinary wave cutoff has been widely discussed [1,8,9]. The increase of the cutoff density with the electron temperature which was found, is so important that relativistic effects have to be taken into account when analysing the results of millimeter wave Thomson scattering, reflectometry or EC emission. Simple expressions for the real part of the refractive index of the ordinary wave

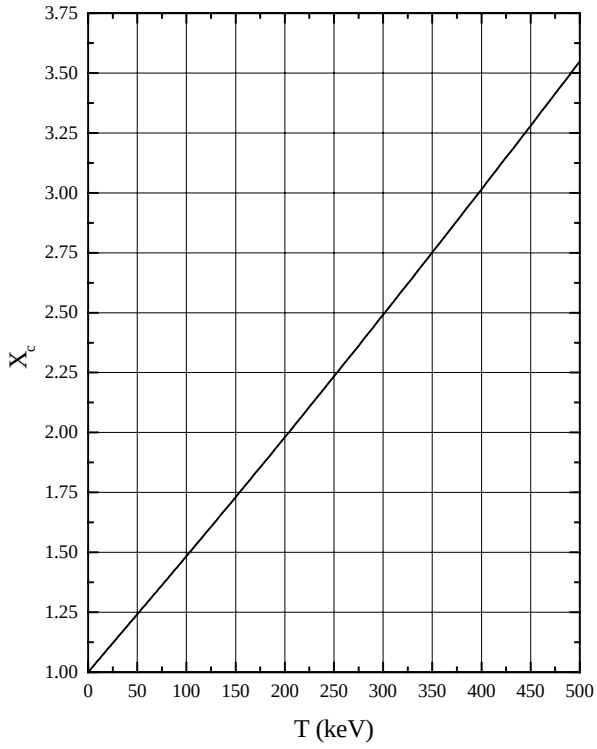

FIG. 1. Cutoff density X_c of ordinary waves versus the electron temperature.

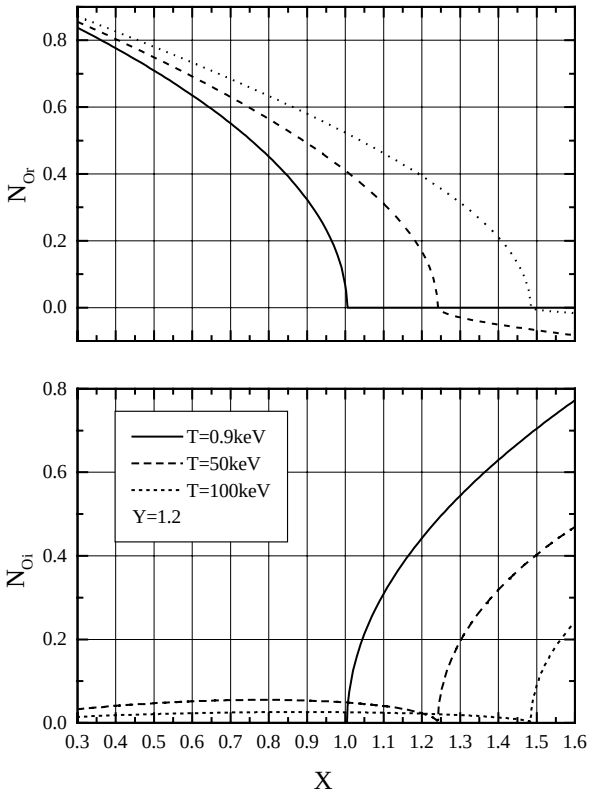

FIG. 2. Variation of the real (N_{Or}) and imaginary (N_{Oi}) part of the ordinary wave refractive index with X for $Y = 1.2$ and $T = 0.9$ keV, $T = 50$ keV and $T = 100$ keV.

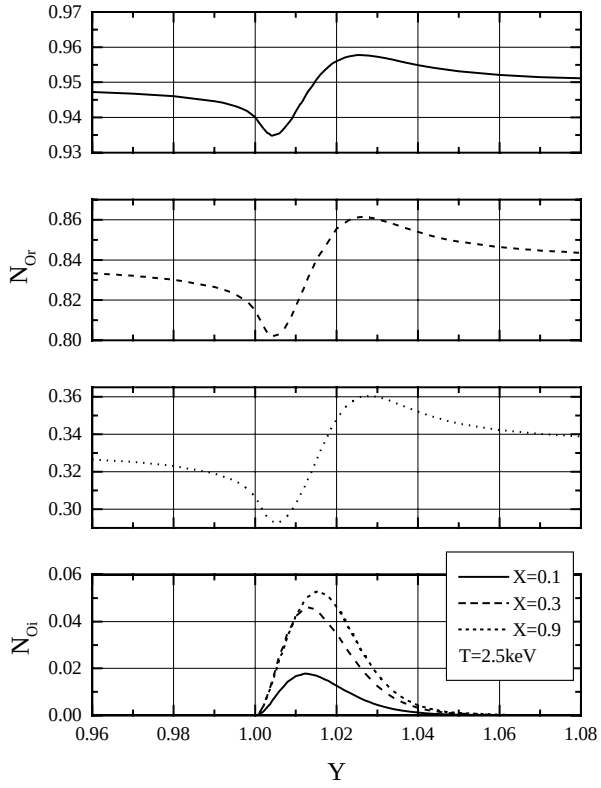

FIG. 3. The real (N_{Or}) and imaginary (N_{Oi}) part of the ordinary wave refractive index versus Y for $T = 2.5$ keV and $X = 0.1$, $X = 0.3$ and $X = 0.9$.

which hold for frequencies far away from the fundamental EC frequency and its first few harmonics, and in a limited range of electron temperature have been also reported [10,11]. Here, in Fig. 1 we present the variation of the cutoff density X_c with the electron temperature up to highly relativistic electron temperatures ($T = 500$ keV). Note that the location of the cutoff density does not depend on Y. One concludes that the increase of the electron temperature leads to a significant increase of X_c. The cutoff density may reach its triple or quadruple cold plasma value (for instance, for $T = 500$ keV one has $X_c \approx 3.55$). This may be attractive for future applications of ordinary waves in fusion devices with high temperatures.

We shall illustrate the dependence of the refractive index of ordinary waves on electron density by representing on Fig. 2 the variation of the real and imaginary part of N_O with density for $Y = 1.2$ and several values of the electron temperature: 0.9 keV, 50 keV and 100 keV. As one might guess, the real part of the wave refractive index N_{Or} decreases for increasing the electron density. The magnetic field or more precisely, Y slightly affects the variation of N_{Or} with X. We note that up to the cutoff density, the curve depicted for $T = 0.9$ keV coincide with that represented in Fig. 8 in [1]. The variation of the imaginary part of the wave refractive index N_{Oi} with X up to the cutoff density, shows a large maximum. For $X \geq X_c$ a wave evanescence region establishes: further increase of the electron density leads to an abrupt increase of N_{Oi}. Simultaneously, instead of vanishing, the real part of the wave refractive index takes small negative values. So, in relativistic plasmas, the classical pure evanescent waves ($N_{Oi} \geq 0$, $N_{Or} = 0$) beyond the cutoff are replaced by highly damped long-wavelength outgoing waves.

Let us now examine the variation of the wave refractive index with Y around the fundamental EC frequency and its first three harmonics. On Fig. 3 we show the real and imaginary part of N_O versus Y for a relatively low ("nonrelativistic") electron temperature 2.5 keV and several values of the electron density: $X = 0.1$, $X = 0.3$ and $X = 0.9$. As expected, near the ECR the wave refractive index varies strongly and at the high field side of the resonance two marked extrema appear. For

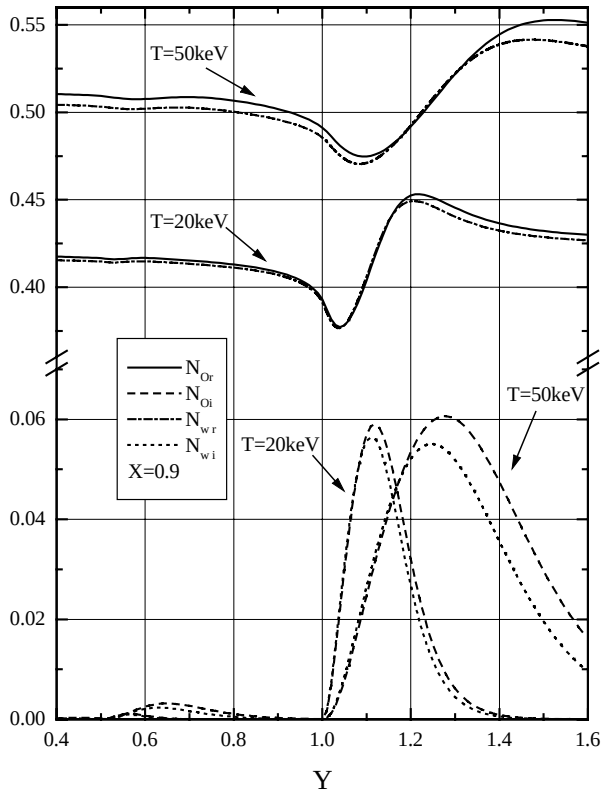

FIG. 4. Comparison of the fully relativistic results with the weakly relativistic ones for $X = 0.9$, $T = 20$ keV and $T = 50$ keV.

increasing the electron density the magnitude of the "wiggle" enlarges. As the electron temperature is reduced the frequency range over which the "wiggle" occurs decreases so that in the limit $T \to 0$, the classical cold plasma behaviour of ordinary waves is recovered (with the exception of the EC frequency itself). It turns out that the basic requirements concerning the applicability of the WKB approximation are more easily violated in low temperature plasmas. At the immediate vicinity of the ECR, in the high field side of the resonance, the solution of (10) becomes complex indicating that ordinary waves propagating perpendicularly to the magnetic field can be effectively damped. For increasing the electron density, the maximum value of N_{Oi} increases and displaces towards higher Y-values. At high densities the damping of ordinary waves near the ECR becomes very efficient (for instance, for $X = 0.9$ one has $N_{Oi} \sim N_{Or}/10$).

The results presented in Fig. 3 as well as those obtained for much lower electron temperatures ($T \geq 0.01$ keV) demonstrate that the applied numerical procedure gives correct results even far away from the relativistic temperature domain. An excellent agreement is found when the results of Fig. 3 are compared with those obtained by using the weakly relativistic numerical code. For higher electron temperatures ($T = 20$ keV and $T = 50$ keV) a comparison with the weakly relativistic results is depicted in Fig. 4. One concludes that for $T = 20$ keV that is, at the boundary of validity of the weakly relativistic approximation, a fairly good agreement is obtained. At higher electron temperatures, both the real and imaginary part of N_O calculated by using the weakly relativistic dispersion relation start to differ significantly, particularly at the high field side of the resonance.

The propagation and absorption properties of ordinary waves around the fundamental EC frequency and its first few harmonics in the high temperature domain are depicted on Fig. 5- 7 on which we show the variation of N_{Or} and N_{Oi} on Y for several values of X ($X = 0.1$, $X = 0.3$ and $X = 0.9$) and $T = 50$ keV (Fig. 5), $T = 100$ keV (Fig. 6) and $T = 300$ keV (Fig. 7). The main features of the ordinary wave propagation and absorption can be summarized as follows:

- In the relativistic temperature domain small "wiggles" appear also around the second and third

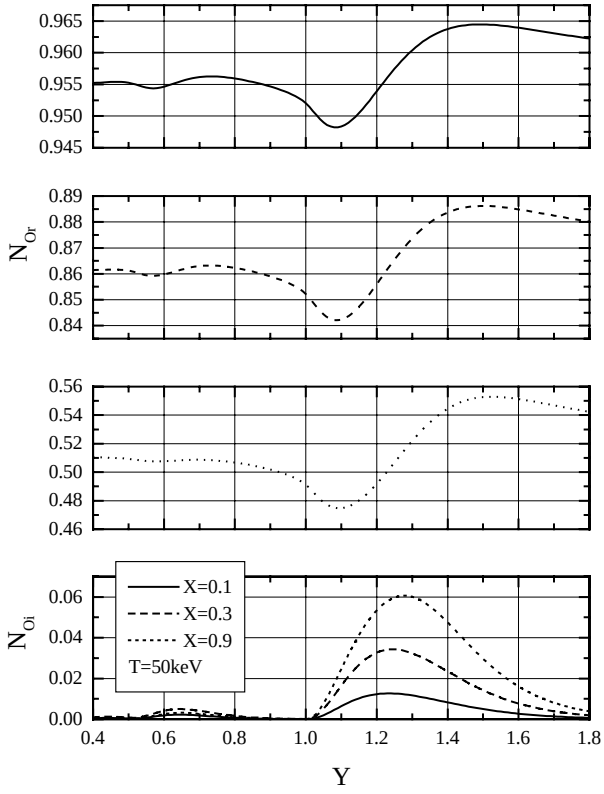

FIG. 5. As in Fig. 3 for T = 50 keV.

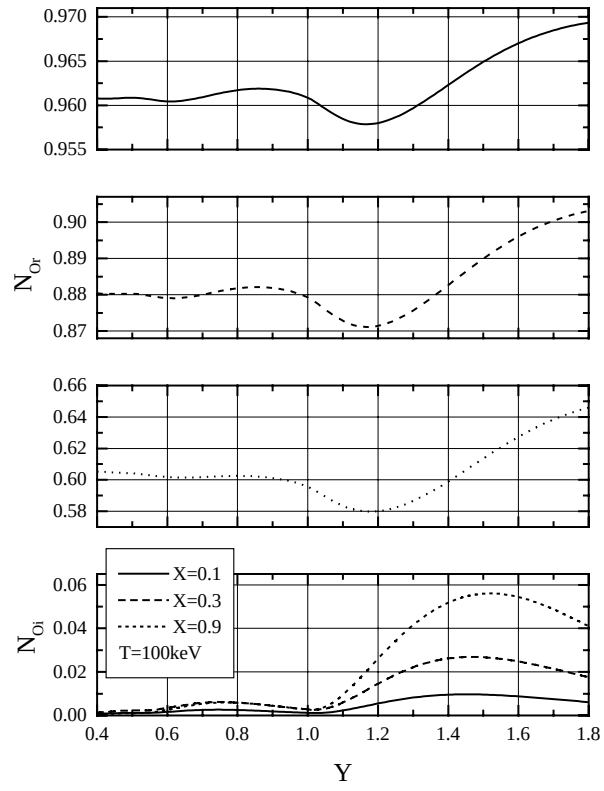

FIG. 6. As in Fig. 3 for T = 100 keV.

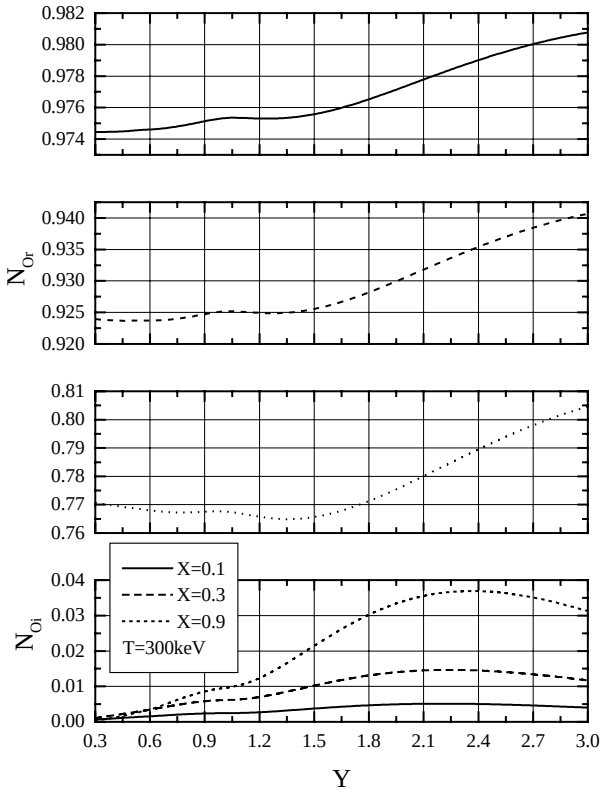

FIG. 7. As in Fig. 3 for T = 300 keV.

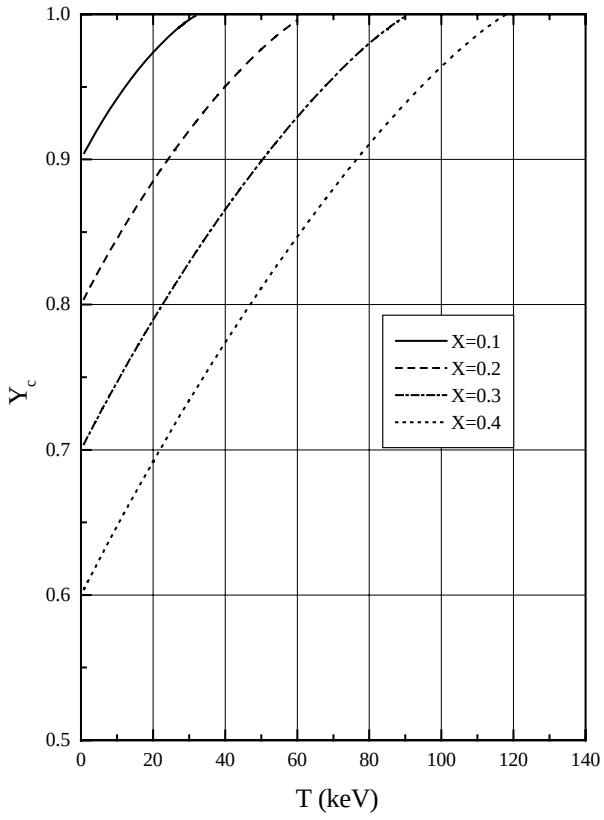

FIG. 8. Temperature dependence of the Y_c value at the right-hand cutoff for several electron densities.

harmonic of the EC frequency. As the electron temperature increases, relativistic effects broaden the cyclotron harmonic resonances so that the magnitude of the "wiggles" decreases and the frequency range over which they occur, enlarges. So, as the relativistic electron mass increases, the anomalous dispersion structures around the fundamental EC frequency and its second and third harmonics gradually disappear (see for instance, the dispersion curves for $T = 300$ keV represented on Fig. 7).

- Generally, the real part of the ordinary wave refractive index enlarges with increasing the electron temperature. In the high temperature range in which the anomalous dispersion structure is washed out, N_{Or} enlarges appreciably with increasing Y beyond the ECR and reaches gradually its free space value ($N_{Or} = 1$).

- The damping of ordinary waves increases with increasing the electron density up to the cutoff density. As the the electron temperature is increased, the maxima of N_{Oi} broaden and displace towards higher Y-values (note for instance, that for $T = 300$ keV and $X = 0.9$, the maximum EC wave absorption takes place at $Y = 2.36$). The broadening of the absorption profiles with the increase of T is so important that at high temperatures a quasi-continuous absorption profiles are obtained (see, for instance, the variation of N_{Oi} with Y for $T = 300$ keV represented on Fig. 7).

IV Extraordinary wave

As is well known (see for example [12]), four characteristic frequencies characterize the range of extraordinary wave propagation: the right- and left-hand cutoff frequencies and the upper and lower hybrid (resonant) frequencies. Since we are interested in the wave propagation and absorption features around the EC frequency and its harmonics, we shall be mainly concerned with the high-frequency range that is, with the right-hand cutoff frequency and the upper hybrid frequency. The cutoffs of the extraordinary wave are given by the roots of the numerator of the right hand side of equation (11) that is, by $N_X^2 = 0$. In the framework of the cold plasma approximation the root describing the right-hand cutoff can be simply expressed as,

$$X_c + Y_c = 1. \tag{13}$$

In thermal plasma however the location of the right-hand cutoff of the extraordinary wave depends on the electron temperature. The temperature dependence of the right hand cutoff is depicted on Fig. 8 on which we show the variation of Y_c with the electron temperature at the location of cutoff for several values of X_c that is, of the electron density. Relativistic effects increase the magnetic field at which the wave is cut off. As may be seen in Fig. 8 for the right-hand cutoff, the largest relative shift occurs near the EC frequency. This has important implications on several plasma diagnostics (e.g. reflectometry, milimeter wave Thomson scattering, etc.).

In Fig. 9, we show the variation of the real and imaginary part of two least damped modes which represent the solutions of the dispersion equation (11) with Y, for $X = 0.2$ and $T = 10$ keV. Obviously, below the right-hand cutoff that is, for $Y \leq Y_c$ the solution labelled N_1 represents the extraordinary electromagnetic wave. The solution labelled N_2 represents a heavily damped electrostatic mode which is of little practical importance. One concludes that the inclusion of relativistic thermal effects leads to major departures from the classical cold plasma wave propagation picture. Namely, near the second harmonic of the EC frequency the extraordinary wave has an anomalous wave dispersion that is, a small "wiggle" of N_r appears near the second harmonic One also notes that wave damping becomes significant near the second ECR harmonic. As the electron density is increased both, the magnitude of the "wiggle" and the wave damping increases up to some critical value X_{CR} at which the solution describing the electromagnetic and electrostatic modes coalesce. For $X > X_{CR}$ the low- and high-field branches of these modes interchange and wave coupling occurs: the low-field branch of the X wave

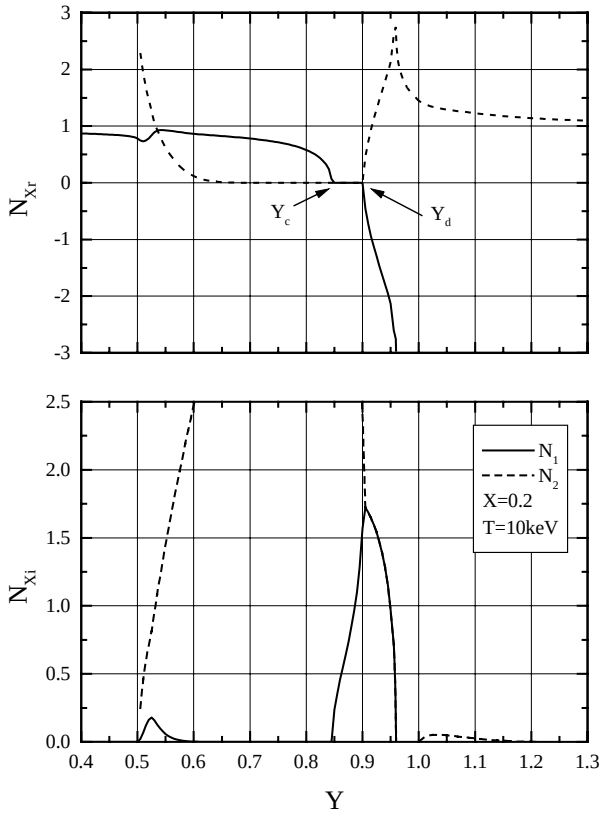

FIG. 9. The real (N_{Xr}) and imaginary part (N_{Xi}) of the wave refractive index of two least damped modes versus Y for X = 0.2 and T = 10 keV.

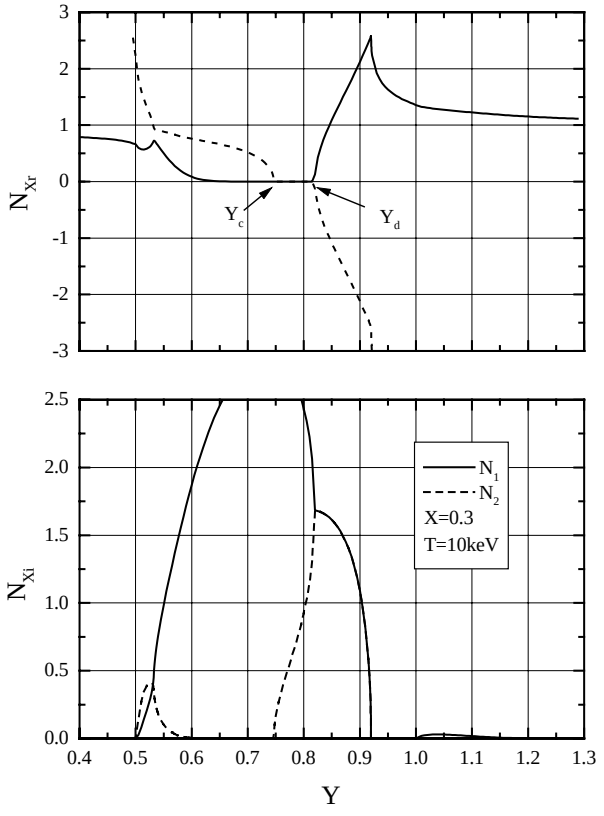

FIG. 10. As in Fig. 9 for X = 0.3.

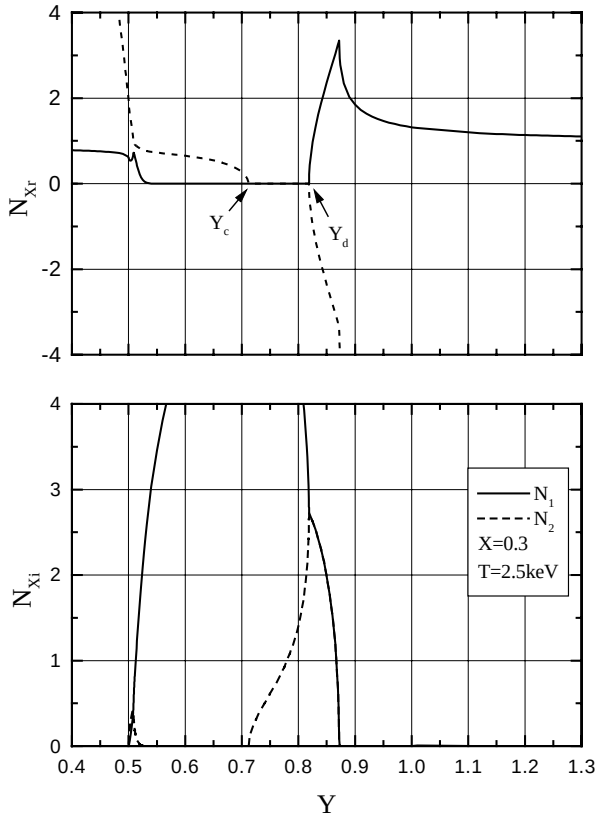

FIG. 11. As in Fig. 10 for $T = 2.5$ keV.

matches smoothly with the highly damped high-field branch of the electrostatic mode while the low-field branch of the electrostatic wave links with the solution trajectory of the electromagnetic wave. The described physical picture of mode interaction is illustrated in Fig. 10 on which we show the variation of N_r and N_i with Y for $X = 0.3$ and the same electron temperature as in Fig. 9, $T = 10$ keV. The parameter which weighs the influence of mode coupling depends on X and T. For $T = 10$ keV one has $X_{CR} = 0.287$. The phenomenon of mode coupling near the second harmonic of the EC frequency has been analysed within the weakly relativistic approximation in [13,14], for perpendicular wave propagation and in [15], for oblique wave propagation. The results obtained in the present fully relativistic analysis confirm and complement the previously reported results on this phenomenon.

Let us now come back to the range beyond the right-hand cutoff $Y > Y_c$. After the right-hand cutoff the solutions of the dispersion equation (11) describe evanescent waves ($N_r = 0$, $N_i \neq 0$). From the upper hybrid resonance which is defined simply by the relation

$$X_d + Y_d^2 = 1 \tag{14}$$

up to point labelled Y_e only the real parts of the solutions describing the electromagnetic and electrostatic modes differ while their imaginary parts are identical. We recall that in the undercritical regime represented in Fig. 9 the electromagnetic wave is labelled N_2 while in the overcritical one on Fig. 10, it is labelled N_1. It turns out that both, the electromagnetic and the electrostatic modes are highly damped in the vicinity of the upper hybrid resonance. The refractive index of the electromagnetic mode has a marked peak at Y_e after which it decreases and joins smoothly the classical solution trajectory of the extraordinary wave. One also notes the EC wave damping near the ECR.

Now, when at fixed electron density the electron temperature changes, one goes from one regime of mode coupling to the other that is, from the overcritical case to the undercritical one, and vice versa. In Fig. 11 we show the same variation as in Fig. 10 but for an electron temperature $T = 2.5$ keV. As one can see, the physical picture which characterizes the overcritical regime is obtained.

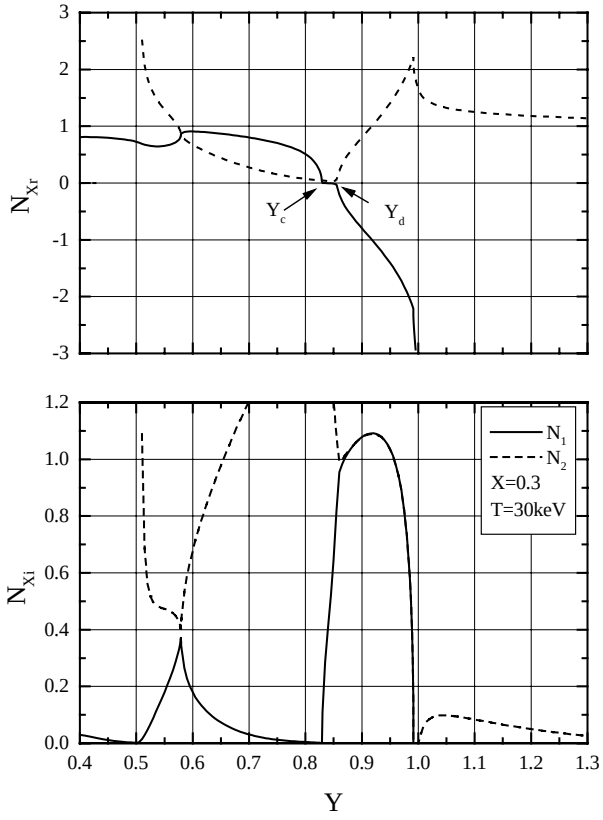

FIG. 12. As in Fig. 11 for T =30 keV.

The only significant difference is the peak at Y_e which becomes very pronounced and large at low temperatures. On the contrary, for increasing the electron temperature one can reach the parameter range in which the undercritical regime establishes. This is illustrated in Fig. 12 in which we show the same variation as in Fig. 10 but for higher electron temperature, $T = 30$ keV. Due to the higher temperature value, the location of the right-hand cutoff Y_c is displaced towards the upper hybrid resonance. As a consequence, the region of wave evanescence is very narrow. One also notes that the absorption profiles at the first, second and third EC harmonics broaden.

Further increase of the electron temperature leads to disappearance of the wave evanescence region. For $X = 0.3$ this occurs at $T = 52$ keV, the case just represented in Fig. 13 Both, the electromagnetic and electrostatic mode are cutoff at one point only, $Y = Y_c$. The wave damping at the upper hybrid resonance combines with the damping at the fundamental EC frequency, and form a single absorption profile. At higher electron temperatures only one mode has a cutoff: the electrostatic mode. This can be further verified in Fig. 14 in which we show the same variation as if Fig. 13 but for $T = 100$ keV. As one can see the highly damped electrostatic mode is cut off at the ECR. On the other side, a continuous absorption profile of the electromagnetic wave in a wide frequency range is obtained. The imaginary part of the wave refractive index however, shows an abrupt increase at the ECR. It should be noted that the wave damping is very efficient. Values of N_i which are comparable to N_r are obtained. Finally at very high electron temperatures, the extraordinary wave becomes almost independent of the magnetic field. In Fig. 15 we show the same variation as in Fig. 14 but for T =300 keV. We see that the wave refractive index of the extraordinary wave is smooth. For increasing Y, the real part of the wave refractive index gradually approaches its free space value.The damping is weak and all harmonic structure is washed out.

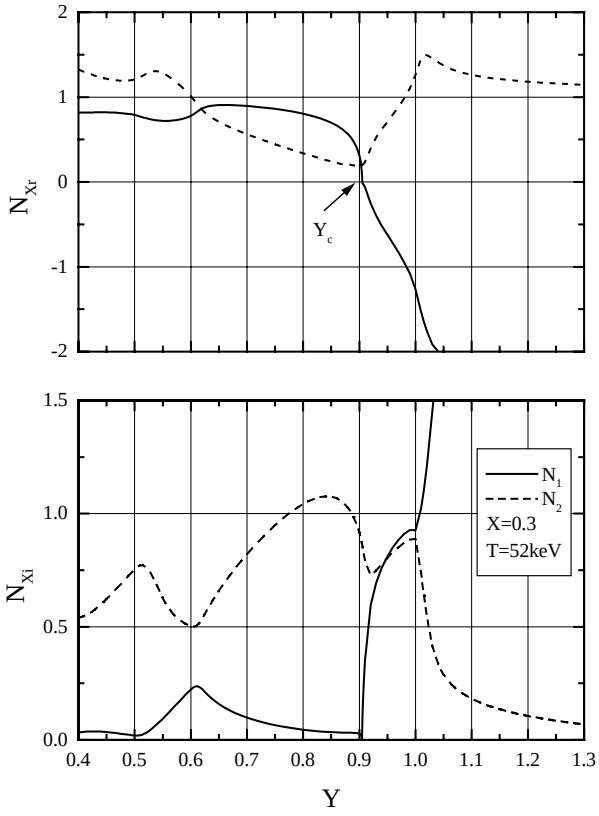

FIG. 13. As in Fig. 12 for T = 52 keV.

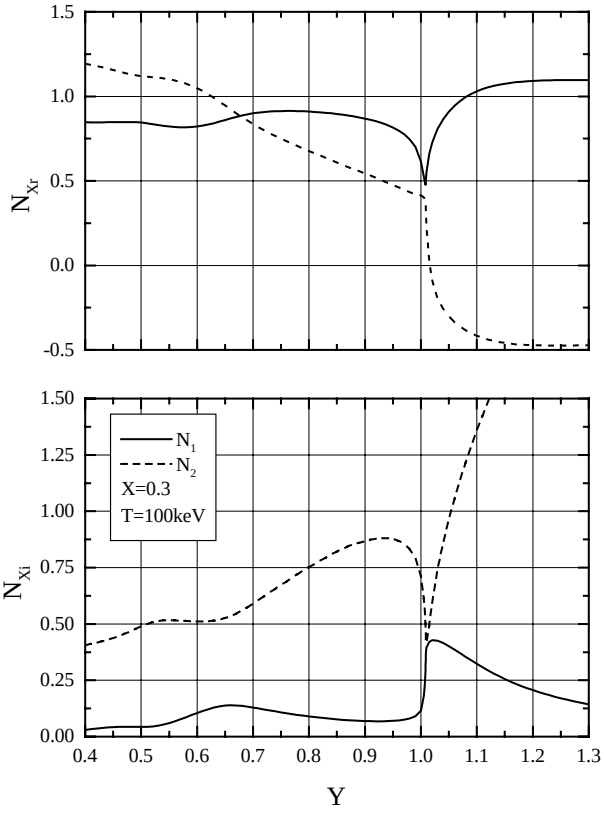

FIG. 14. As in Fig. 13 for T = 100 keV.

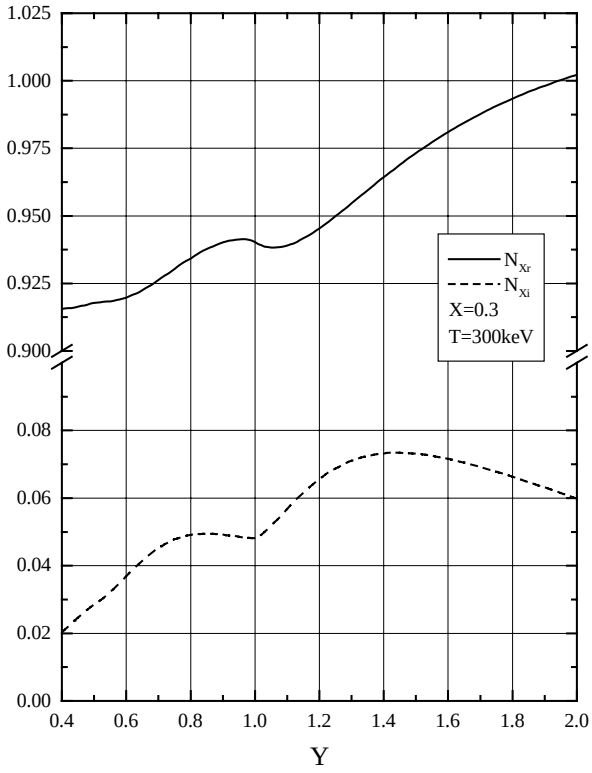

FIG. 15. As in Fig. 14 for T = 300 keV.

V Conclusions

We have investigated ordinary and extraordinary waves propagating perpendicularly to the stationary magnetic field in relativistic plasmas. The relativistic mass increase associated with increasing the electron temperature introduces several interesting effects. In the range of fully relativistic temperatures the cutoff density of ordinary waves is significantly enlarged; double to quadruple cold plasma cutoff density values are obtained for temperatures in the range T = 200 - 500 keV. Beyond the cutoff density, long-wavelength highly-damped oscillations arise. Significant deviations in the real part of the wave refractive index from the cold plasma value are found. Generally, as the electron temperature is increased N_{Or} enlarges. However, the effects of anomaluos wave dispersion which appear near the fundamental EC frequency and its second and third harmonic, are largest for low electron temperatures. For increasing T, the frequency range over which the "wiggles" occur gradually enlarges and their magnitude reduces. It should be pointed out that the effects of anomalous wave dispersion subsist up to the intermediate temperatures ($T \approx 300$ keV). Simultaneously, the harmonic structure of the wave absorption profiles is washed out. An efficient damping of ordinary waves are obtained in a wide temperature range. It increases with increasing the electron density. As the electron temperature is increased, the maxima of the imaginary part of the wave refractive index broden and displace towards higher Y - values. So, the anomalous wave dispersion effects and the harmonic structure of the absorption profile almost simultaneously disappear.

Relativistic effects increase the magnetic field at which the extraordinary wave is cut off. The largest relative shifts of the location of the right-hand cutoff occurs near the electron cyclotron frequency. In the range of intermediate electron temperatures, the right-hand cutoff of the extraordinary wave disappears. The phenomenon of mode coupling near the second harmonic of the electron cyclotron frequency is examined in details, in a wide electron density and temperature ranges. The results of the present fully relativistic analysis confirm and complement the previously reported ones on this phenomenon. Both, the electromagnetic and electrostatic modes are efficient damped near the

upper hybrid resonance.

In summary, the results obtained may have important implications for the wave absorption and in particular, emission in relativistic plasmas. Also, they indicate interesting features of ordinary and extraordinary waves propagating in relativistic plasmas which may be attractive for future applications in devices with high electron temperatures.

References

[1] D.B. Batchelor, R.C. Goldfinger and H. Weitzner, Physics Fluids **27** (1984) 2835.

[2] M. Bornatici, R. Cano, O. De Barbieri and F. Engelmann, Nucl. Fusion **23** (1983) 1153.

[3] I. Weiss, J. Comput. Phys. **61** (1985) 403.

[4] Lj. Nikolić, S. Pešić and N. Oklobdžija, XLI Conf. ETRAN, to be published (1997).

[5] S. Pešič, Lj. Nikolić and N. Oklobdžija, Proc. 3rd General Conf. Balkan Phys. Union, to be published (1997).

[6] B.A. Trubnikov, in Plasma Physics and the Problem of Thermonuclear Reactions (Leontovich M.A., Ed.) Vol. **3**, Pergamon Press, London, (1959) 122.

[7] I.P. Shkarofsky, Physics Fluids **9** (1966) 561.

[8] P.A. Robinson, J. Plasma Physics **37** (1987) 435.

[9] J. Egedal and H. Bindslev, Plasma Phys. Control. Fusion **36** 1994) 543.

[10] H. Bindslev, Plasma Phys. Contr. Fusion **34** (1992) 1601.

[11] E. Mazzucato, Physics Fluids **B4** (1992) 3460.

[12] S. Pešić, in Waves in Plasmas, INN Vinča (1997), to be published.

[13] E. Lazzaro and G. Ramponi, Plasma Phys. **23** (1981) 53.

[14] M. Bornatici, F. Engelmann, C. Maroli and V. Petrillo, Plasma Phys. **23** (1981) 89.

[15] S. Pešić, Phys. Fluids **31** (1988) 122.

(Received November 1997.)